DISPERSIVE PROPERTIES OF GROUNDED SLOTLINES AND EDGE COUPLED MICROSTRIP LINES ON BIAXIAL SUBSTRATES

T Q Ho and B Beker
Department of Electrical and Computer Engineering
University of South Carolina
Columbia, SC 29208

ABSTRACT

The spectral domain analysis is applied to study the propagation characteristics of grounded slotlines and edge coupled microstrip lines on biaxial substrates The formulation derives an expression for the Green's function which is valid for substrates simultaneously specified by both their permittivity and permeability tensors The behavior of the normalized wavelength, index of refraction, and propagation constant are examined in detail with respect to different line width / substrate thickness ratios as well as the material parameters Some of the numerically calculated data describing propagation characteristics of these structures are presented here for the first time.

I. INTRODUCTION

With recent development of MIC and MMIC technologies, the concept of designing components using anisotropic materials seems to attract the attention of many circuit designers. In order to accurately construct these components, dispersive properties of the transmission lines must be known, otherwise extensive tuning may be required at a later time to achieve desired performance. The solution to various transmission line structures on some anisotropic substrates are well documented [1-6], however, the major effort has been devoted toward structures on uniaxial substrates only Up until now, there seems to be no data available on propagation characteristics for cases involving grounded slotlines and edge coupled lines on biaxial substrates In this paper, an analysis based on the spectral domain method is applied to examine the propagation properties of these two structures. The problem is generalized so that both dielectric and magnetic anisotropy are included in the formulation. The Green's functions for both structures are derived through the transformed wave equations which reduce to a set of fourth order uncoupled differential equations. An algorithm based on Galerkin's method is then developed and used to compute the propagation constant, index of refraction, and normalized wavelength Using the newly developed expression for the Green's function, the propagation constant of a line on the uniaxial substrate, which is treated as a special case of its biaxial counterpart, is computed and compared to the existing data. The comparison shows an excellent agreement throughout the chosen frequency range. The dispersive properties of the grounded slotlines and edge coupled microstrip lines on biaxial substrates are then examined in detail. Numerous cases are treated with respect to different geometrical and medium parameters, with data tabulated for frequencies up to 40 0 GHz. In addition, an example is given to illustrate the anisotropic effect on the index of refraction when grounded slotlines are printed on a substrate for which both [ε] and [μ] tensors are simultaneously specified.

II THEORY

Consider the geometry of Fig. (1) which illustrates the cross section of the grounded slotline and edge coupled microstrips. The metal strips are taken to be perfectly conducting and infinitely thin. The substrate with thickness h_1 is lossless, and is generally characterized by its biaxial permittivity and permeability tensors,

$$[\varepsilon] = \varepsilon_0 \begin{vmatrix} \varepsilon_{xx} & \varepsilon_{xy} & 0 \\ \varepsilon_{yx} & \varepsilon_{yy} & 0 \\ 0 & 0 & \varepsilon_{zz} \end{vmatrix} \quad \text{and} \quad [\mu] = \mu_0 \begin{vmatrix} \mu_{xx} & 0 & 0 \\ 0 & \mu_{yy} & 0 \\ 0 & 0 & \mu_{zz} \end{vmatrix} \tag{1a}$$

with

$$\varepsilon_{xx} = \varepsilon_2 \sin^2(\theta) + \varepsilon_1 \cos^2(\theta), \quad \varepsilon_{yy} = \varepsilon_2 \cos^2(\theta) + \varepsilon_1 \sin^2(\theta)$$
$$\varepsilon_{zz} = \varepsilon_3, \quad \varepsilon_{xy} = \varepsilon_{yx} = (\varepsilon_2 - \varepsilon_1)\sin(\theta)\cos(\theta) \tag{1b}$$

where ε_0 and μ_0 are the free-space permittivity and permeability, respectively The angle θ is the rotation angle of the principle axes with respect to the coordinate axes of the structure For simplicity, this analysis will only consider two special cases of rotation One is when θ equals to 0^o and the other is when θ equals to 90^o Under these conditions, the ε_{xy} and ε_{yx} elements are zero.

The vector wave equations for the components of the electric and magnetic fields within the biaxial substrates can be written in their compact forms as,

$$\nabla \times (\bar{\bar{\mu}}^{-1} \cdot \nabla \times \vec{E}) - k_0^2 \bar{\bar{\varepsilon}} \cdot \vec{E} = 0 \tag{2a}$$
$$\nabla \times (\bar{\bar{\varepsilon}}^{-1} \cdot \nabla \times \vec{H}) - k_0^2 \bar{\bar{\mu}} \vec{H} = 0 \tag{2b}$$

where $[\varepsilon]$ and $[\mu]$ are previously defined in equation (1) and k_0 is the free-space wave number.

When the Fourier transform of any field component is defined as

$$\tilde{\Phi}(x,\alpha) = \int_{-b/2}^{b/2} \Phi(x,y)\, e^{j\alpha y}\, dy \tag{3}$$

with α being the discrete Fourier transform variable, equations (2a,b) reduce to a set of fourth order uncoupled differential equations and written as,

$$(\partial^4/\partial x^4)\tilde{E}_z + \chi_1(\partial^2/\partial x^2)\tilde{E}_z + \chi_2 \tilde{E}_z = 0 \tag{4a}$$
$$(\partial^4/\partial x^4)\tilde{E}_y + \chi_1(\partial^2/\partial x^2)\tilde{E}_y + \chi_2 \tilde{E}_y = 0 \tag{4b}$$

with,

$$\chi_1 = k_0^2(\varepsilon_{zz}\mu_{yy} + \varepsilon_{yy}\mu_{zz}) - \beta^2(\varepsilon_{zz}/\varepsilon_{xx} - \mu_{zz}/\mu_{xx}) - \alpha^2(\mu_{yy}/\mu_{xx} + \varepsilon_{yy}/\varepsilon_{xx}) \tag{4c}$$
$$\chi_2 = \{(k_0^2\mu_{yy}\varepsilon_{zz} - \beta^2\varepsilon_{zz}/\varepsilon_{xx} - \alpha^2\mu_{yy}/\mu_{xx})(k_0^2\mu_{zz}\varepsilon_{yy} - \beta^2\mu_{zz}/\mu_{xx} - \alpha^2\varepsilon_{yy}/\varepsilon_{xx}) - (\alpha\beta)^2(\mu_{yy}/\mu_{xx} - \varepsilon_{yy}/\varepsilon_{xx})(\mu_{zz}/\mu_{xx} - \varepsilon_{zz}/\varepsilon_{xx})\} \tag{4d}$$

so that χ_1 and χ_2 are the transformed coefficients which are dependent on tensor elements as well The general solutions to equations (4a,b) are sinusoidal forms which represent the standing waves in regions 1 and 2. By applying the appropriate boundary conditions at the interface $x = h_1$, a set of matrix equations can be formed, yielding the expression for the admittance Green' s function given below

$$\begin{vmatrix} \tilde{Y}_{yy}(\alpha,\beta) & \tilde{Y}_{yz}(\alpha,\beta) \\ \tilde{Y}_{zy}(\alpha,\beta) & \tilde{Y}_{zz}(\alpha,\beta) \end{vmatrix} \begin{vmatrix} \tilde{E}_y(\alpha) \\ \tilde{E}_z(\alpha) \end{vmatrix} = \begin{vmatrix} \tilde{J}_{ys}(\alpha) \\ \tilde{J}_{zs}(\alpha) \end{vmatrix} \tag{5a}$$

with system matrix elements defined by

$$\tilde{Y}_{yy}(\alpha,\beta) = \xi_8\Psi^2 + \{\xi_4\Psi^{1a} - \xi_3\Psi^{1b}\}/\xi_{11} \quad (5b)$$

$$\tilde{Y}_{zy}(\alpha,\beta) = -\xi_7\gamma_2 + \{\xi_2\Psi^{1a} - \xi_1\Psi^{1b}\}/\xi_{10} \quad (5c)$$

$$\tilde{Y}_{yz}(\alpha,\beta) = -\xi_7\gamma_2 + \{\xi_4\xi_5\Psi^{1a} - \xi_3\xi_6\Psi^{1b}\}/\xi_{11} \quad (5d)$$

$$\tilde{Y}_{zz}(\alpha,\beta) = \xi_9\gamma_2 + \{\xi_2\xi_5\Psi^{1a} - \xi_1\xi_6\Psi^{1b}\}/\xi_{10} \quad (5e)$$

$$\Psi^2 = \coth(\gamma_2 h_2), \quad \Psi^{1a} = \tan(\gamma^{1a} h_1), \quad \Psi^{1b} = \tan(\gamma^{1b} h_1) \quad (5f,g,h)$$

Here, β is the propagation constant in the z direction, γ^{1a}, γ^{1b} and γ_2 are propagation constants in the x direction within region 1 and 2, respectively. The remaining constants appearing above, ξ_1 to ξ_{11}, can be written in terms of χ_1 and χ_2.

The spectral domain method for computing the propagation constant is outlined in the following sections for the grounded slotline and the edge coupled microstrip line.

Grounded slotline:

An application of the Galerkin method in the Fourier domain along with Parseval's theorem [7-8] to equation (5a), allows for a set of algebraic equations to be derived in the following form,

$$\sum_{m=1}^{M} K_{im}^{(1,1)} C_m + \sum_{m=1}^{N} K_{im}^{(1,2)} D_m = 0 \qquad i = 1,2,3,\ldots N \quad (6a)$$

$$\sum_{m=1}^{M} K_{im}^{(2,1)} C_m + \sum_{m=1}^{N} K_{im}^{(2,2)} D_m = 0 \qquad i = 1,2,3,\ldots M \quad (6b)$$

wherein the matrix elements are

$$K_{im}^{(1,1)} = \sum_{n=1}^{\infty} \tilde{E}_{yi}(n)\,\tilde{Y}_{yy}(n,\beta)\,\tilde{E}_{ym}(n) \quad (7a)$$

$$K_{im}^{(1,2)} = \sum_{n=1}^{\infty} \tilde{E}_{yi}(n)\,\tilde{Y}_{yz}(n,\beta)\,\tilde{E}_{zm}(n) \quad (7b)$$

$$K_{im}^{(2,1)} = \sum_{n=1}^{\infty} \tilde{E}_{zi}(n)\,\tilde{Y}_{zy}(n,\beta)\,\tilde{E}_{ym}(n) \quad (7c)$$

$$K_{im}^{(2,2)} = \sum_{n=1}^{\infty} \tilde{E}_{zi}(n)\,\tilde{Y}_{zz}(n,\beta)\,\tilde{E}_{zm}(n) \quad (7d)$$

the transverse and the longitudinal components of the electric field across the slot $\tilde{E}_y$ and $\tilde{E}_z$ can be expanded in terms of the known basis functions, so that numerical solution of simultaneous equation (6) provides the propagation constant β, which is obtained by setting the determinant of the coefficient matrix equal to zero and searching for the root of the resulting secular equation.

Edge coupled microstrip line:

The procedure used to solve for β in the case of the coupled microstrip line is similar to the one applied to the grounded slotline, except here, we deal with the impedance Green's function and the current basis functions on the metal strips. The matrix elements in this case are given by

$$K_{im}^{(1,1)} = \sum_{n=1}^{\infty} \tilde{J}_{zi}(n)\,\tilde{Z}_{zz}(n,\beta)\,\tilde{J}_{zm}(n) \quad (8a)$$

$$K_{im}^{(1,2)} = \sum_{n=1}^{\infty} \tilde{J}_{zi}(n)\,\tilde{Z}_{zy}(n,\beta)\,\tilde{J}_{ym}(n) \quad (8b)$$

$$K_{im}^{(2,1)} = \sum_{n=1}^{\infty} \tilde{J}_{yi}(n)\,\tilde{Z}_{yz}(n,\beta)\,\tilde{J}_{zm}(n) \quad (8c)$$

$$K_{im}^{(2,2)} = \sum_{n=1}^{\infty} \tilde{J}_{yi}(n)\,\tilde{Z}_{yy}(n,\beta)\,\tilde{J}_{ym}(n) \quad (8d)$$

with the individual impedance elements related to their admittance counterparts presented in equation (5)

$$\tilde{Z}_{zz}(\alpha,\beta) = \tilde{Y}_{yy}(\alpha,\beta)/\Delta, \quad \tilde{Z}_{zy}(\alpha,\beta) = -\tilde{Y}_{zy}(\alpha,\beta)/\Delta$$
$$\tilde{Z}_{yz}(\alpha,\beta) = -\tilde{Y}_{yz}(\alpha,\beta)/\Delta, \quad \tilde{Z}_{yy}(\alpha,\beta) = \tilde{Y}_{zz}(\alpha,\beta)/\Delta \quad (8e)$$
$$\Delta = \tilde{Y}_{yy}\tilde{Y}_{zz} - \tilde{Y}_{yz}\tilde{Y}_{zy}$$

Notice that this structure is capable of supporting both even and odd modes, accordingly, appropriate choices for α, $\tilde{J}_z$, and $\tilde{J}_y$ must be chosen during the computation of the propagation constant.

III. RESULTS

To verify the theory and its spectral domain implementation, the dispersive characteristics of the grounded slotline and edge coupled microstrip line on a uniaxial substrate, which is treated as a special case of biaxial substrate, are computed and compared to the existing data. For the grounded slotline, sapphire is used as the substrate material, whereas for the edge coupled microstrip, boron nitride is used instead. Fig. 2a shows the effective dielectric constant computed against k_0, while Fig. 2b shows the responses of normalized β's versus frequency. Plotted also along with our data are the results reproduced from references [4-5], and excellent agreement is observed.

The effects of anisotropy on biaxial substrates are studied with respect to different parameters. The selected substrates are the glass cloth and PTFE cloth. In the first case, the material parameters are $\varepsilon_1 = 6.24$, $\varepsilon_2 = 6.64$, $\varepsilon_3 = 5.56$, and $\mu_{xx} = \mu_{yy} = \mu_{zz} = 1.0$ respectively, and in the second case they are $\varepsilon_1 = 2.45$, $\varepsilon_2 = 2.89$, and $\varepsilon_3 = 2.95$, and $\mu_{xx} = \mu_{yy} = \mu_{zz} = 1.0$. Fig. 3 shows the frequency response of the effective dielectric constant of the grounded slotline on glass cloth under 0^o and 90^o rotation of the permittivity tensor. As the frequency moves into the higher bands, ε_{eff} increases correspondingly. The effective dielectric constant is also seen to increase as θ rotates from 0^o to 90^o. Next, using the same physical dimensions of the structure, the propagation characteristics of the grounded slotline on another biaxial substrate, namely PTFE cloth, are computed and tabulated in table 1. The propagation constant, normalized wavelength, and the effective dielectric constant are documented for different frequencies, and all of them apart from λ_g are tending towards higher values.

The dispersive properties of the edge coupled microstrip lines on glass cloth are calculated and shown in Fig. 4. Here, both even and odd modes are considered. The data indicated that the dielectric constant of the even mode is generally higher than that belonging to the odd mode. This same behavior is normally observed in isotropic substrates. The characteristic parameters β, λ_g, and ε_{eff} of the edge coupled line as function of the line spacing and the strip width are also examined with results tabulated in tables 2,3,4,5 for both even and odd modes, wherein both angles of rotation for $[\varepsilon]$ are also considered. Table 6 shows the tabulated data with the dispersive properties of the coupled microstrip line on PTFE cloth. Here again, results are calculated for frequencies up to 40.0 GHz.

To illustrate how $[\mu]$ elements would change the effective index of refraction, numerical results for the grounded slotline on a substrate that characterized by both its biaxial $[\varepsilon]$ and $[\mu]$ are also presented. Curves A, B, and C of Fig. 5 are computed when all elements in $[\mu]$ are one for different values of the permittivity tensor. Then by changing the material from magnetically isotropic to biaxial, effectively increases the index of refraction. Curve D is for $\mu_{xx} = 1.0$, and $\mu_{yy} = \mu_{zz} = 1.2$ and curve E

corresponds to μ_{xx} = 1.0, μ_{yy} = 1.2, and μ_{zz}=1.97. At lower frequencies, there is almost no difference in the effective index of refraction, however, as frequencies move into millimeter-wave range, the separation between the two cases becomes apparent.

IV. CONCLUSION

The spectral domain method applied to study the dispersive properties of the grounded slotline and the edge coupled microstrip on biaxial substrates is presented. The newly derived Green's function taking into account of both [ε] and [μ] tensors is written explicitly in its closed form. Propagation characteristics are examined when these lines are printed on biaxial substrates, such as the glass cloth and the PTFE cloth. Numerical data are tabulated with respect to different parameters for frequencies up to 40.0 GHz for both 0^o and 90^o rotation of the permittivity tensor. Also, the variation in the index of refraction is examined when the substrate is characterized simultaneously by both its permittivity and permeability tensors. Numerous examples are presented in graphical and tabular forms describing propagation characteristics of two important structures commonly found in practice.

REFERENCES

[1] R.P Owens, J.E. Itken, and T.C. Edwards, "Quasi-static characteristics of microstrip on an anisotropic sapphire substrate," IEEE Trans. Microwave Theory Tech., vol. MTT-24, pp. 499-505, Aug. 1976.

[2] A-M. A. Al-Sherbiny, "Hybrid mode analysis of microstrip lines on anisotropic substrates," IEEE Trans. Microwave Theory Tech., vol. MTT-29, pp. 1261-1265, Dec. 1981.

[3] F. Medina and M. Horno," Determination of Green's function matrix for multiconductor and anisotropic multidielectric planar transmission lines: a variational approach," IEEE Trans. Microwave Theory Tech., vol. MTT-33, pp. 933-940, Oct. 1985.

[4] A.A. Mostafa, C. M. Krowne, and K.A. Zaki,"Numerical Spectral Matrix method for propagation in general layered media: application to isotropic and anisotropic substrates," IEEE Trans. Microwave Theory Tech., vol. MTT-35, pp. 1399-1407, Dec. 1987.

[5] A. Nakatani and N.G. Alexopoulos,"Toward a generalized algorithm for the modeling of the dispersive properties of integrated circuit structures on anisotropic substrates," IEEE Trans. Microwave Theory Tech., vol. MTT-33, pp. 1436-1441, Dec. 1985.

[6] N. G. Alexopoulos,"Integrated Circuit structures on anisotropic substrates," IEEE Trans. on Microwave Theory Tech., vol. MTT-33, pp. 847-881, Oct. 1985.

[7] T. Itoh and R. Mittra,"Spectral domain approach for calculating the dispersion characteristics of microstrip lines," IEEE Trans. on Microwave Theory Tech., vol. MTT-21, pp. 496-499, July 1973.

[8] Y.C. Shih and T. Itoh,"Analysis of transmission lines on semiconductor substrate," Univ. of Texas Microwave Laboratory Report No. 84-2, Mar. 1984.

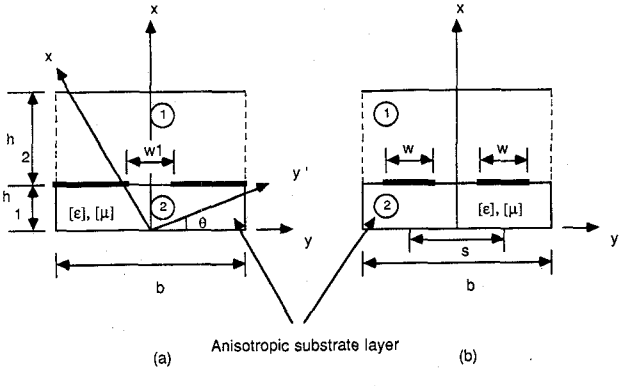

Fig. 1. Geometry of the transmission line on biaxial substrate. (a) Grounded slotline. (b) Edge coupled microstrip line.

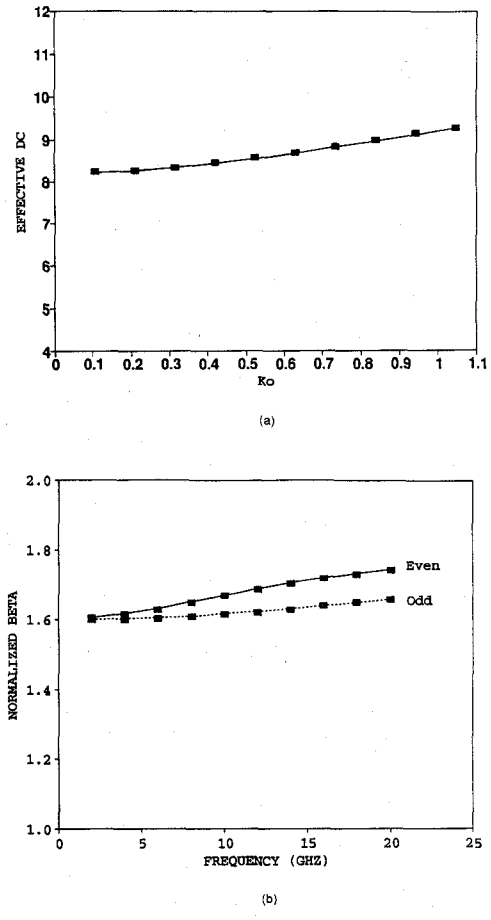

Fig. 2. Dispersion characteristics (a) grounded slotline on sapphire with b =1.0 mm, h_1 = 0.1 mm, h_2 = 0.4 mm, and w_1 = 0.1 mm (b) edge coupled microstrip line on boron nitride with b = 8.5 mm, h_1 = 1.5 mm, h_2 = 3.0 mm, w =1. 5 mm, and s = 3.0 mm. ---------- Data computed by this method. ■ ■ ■ ■ Data reproduced from references [4-5].

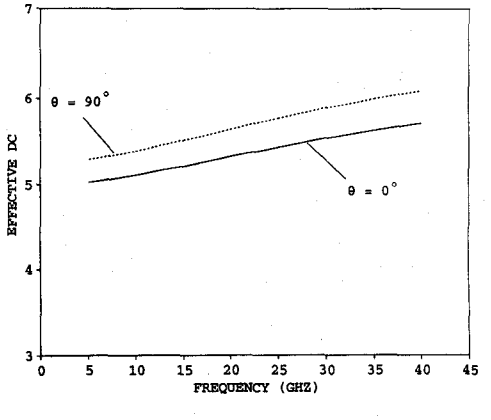

Fig. 3. Effective dielectric constant versus frequency of grounded slotline on glass cloth with ε_1 = 6.24, ε_2 = 6.64, ε_3 = 5.56, and μ_{xx} = μ_{yy} = μ_{zz} = 1.0. The physical dimensions are b = 3.555 mm, h_1 = 0.254 mm, h_2 = 3.301 mm, and w_1 = 0.254 mm.

TABLE 1

Characteristics of grounded slotline on PTFE cloth versus frequency and θ with b = 3.555 mm, h_1 = 0.254 mm, h_2 = 3.301 mm, and w_1 = 0.254 mm.

Freq.	$\beta(0^0)$	$\lambda_g(0^0)$	$\varepsilon_{eff}(0^0)$	$\beta(90^0)$	$\lambda_g(90^0)$	$\varepsilon_{eff}(90^0)$
5.00	0.1524	0.6869	2.1195	0.1627	0.6435	2.4147
10.0	0.3053	0.6858	2.1259	0.3262	0.6419	2.4262
15.0	0.4591	0.6842	2.1360	0.4911	0.6396	2.4440
20.0	0.6140	0.6821	2.1489	0.6578	0.6367	2.4665
25.0	0.7701	0.6798	2.1637	0.8265	0.6335	2.4918
30.0	0.9276	0.6773	2.1795	0.9971	0.6301	2.5185
35.0	1.0862	0.6748	2.1958	1.1695	0.6268	2.5454
40.0	1.2459	0.6723	2.2120	1.3434	0.6235	2.5716

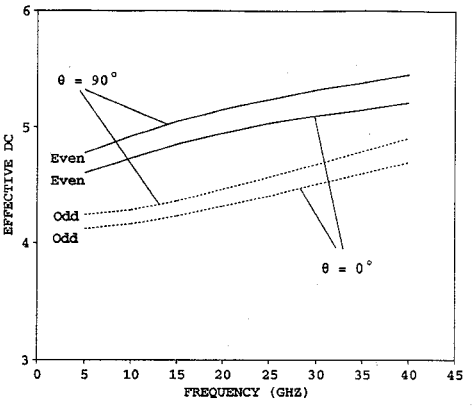

Fig. 4. Effective dielectric constant versus frequency of edge coupled microstrip line on glass cloth with ε_1 = 6.24, ε_2 = 6.64, ε_3 = 5.56, and $\mu_{xx} = \mu_{yy} = \mu_{zz}$ =1.0. The physical dimensions are b = 7.0 mm, h_1 = 0.5 mm, h_2 = 3.0 mm, w =0.5 mm, and s = 1.5 mm.

TABLE 2

Characteristics of coupled line on glass cloth versus s with b = 7.00 mm, h_1 = 0.5 mm, h_2 = 3.0 mm, w = 0.5 mm, θ = 0°, and f = 40.0 GHz.

s	β^e	λ_g^e	ε_{eff}^e	β^o	λ_g^o	ε_{eff}^o
1.00	1.9424	0.4312	5.3762	1.7657	0.4744	4.4422
1.50	1.9133	0.4378	5.2160	1.8163	0.4612	4.7005
2.00	1.8915	0.4428	5.0981	1.8442	0.4542	4.8462
2.50	1.8794	0.4457	5.0332	1.8576	0.4509	4.9169
3.00	1.8731	0.4472	4.9994	1.8633	0.4496	4.9472
3.50	1.8692	0.4481	4.9786	1.8649	0.4492	4.9554

TABLE 3

Characteristics of coupled line on glass cloth versus w/h_1 with b = 7.00 mm, h_1 = 0.5 mm, h_2 = 3.0 mm, s = 1.0 + w, θ = 0°, and f = 40.0 GHz.

w / h_1	β^e	λ_g^e	ε_{eff}^e	β^o	λ_g^o	ε_{eff}^o
0.2	1.8164	0.4612	4.7008	1.7128	0.4891	4.1802
0.4	1.8514	0.4525	4.8838	1.7438	0.4804	4.3328
0.6	1.8766	0.4464	5.0176	1.7706	0.4731	4.4669
0.8	1.8967	0.4417	5.1256	1.7946	0.4668	4.5891
1.0	1.9133	0.4378	5.2161	1.8163	0.4612	4.7006
1.2	1.9274	0.4347	5.2929	1.8358	0.4563	4.8018
1.4	1.9393	0.4319	5.3591	1.8531	0.4521	4.8932

TABLE 4

Characteristics of coupled line on glass cloth versus s with b = 7.00 mm, h_1 = 0.5 mm, h_2 = 3.0 mm, w = 0.5 mm, θ = 90°, and f = 40.0 GHz.

s	β^e	λ_g^e	ε_{eff}^e	β^o	λ_g^o	ε_{eff}^o
1.00	1.9917	0.4206	5.6525	1.7971	0.4661	4.6015
1.50	1.9571	0.4280	5.4577	1.8554	0.4515	4.9049
2.00	1.9333	0.4333	5.3255	1.8857	0.4442	5.0669
2.50	1.9207	0.4361	5.2568	1.8996	0.4410	5.1417
3.00	1.9145	0.4376	5.2227	1.9053	0.4396	5.1727
3.50	1.9108	0.4384	5.2025	1.9068	0.4393	5.1810

TABLE 5

Characteristics of coupled line on glass cloth versus w/h_1 with b = 7.00 mm, h_1 = 0.5 mm, h_2 = 3.0 mm, s = 1.0 + w, θ = 90°, and f = 40.0 GHz.

w / h_1	β^e	λ_g^e	ε_{eff}^e	β^o	λ_g^o	ε_{eff}^o
0.2	1.8451	0.4540	4.8507	1.7325	0.4835	4.2768
0.4	1.8855	0.4443	5.0854	1.7697	0.4734	4.4624
0.6	1.9146	0.4375	5.2232	1.8016	0.4650	4.6248
0.8	1.9379	0.4323	5.3508	1.8300	0.4578	4.7718
1.0	1.9571	0.4280	5.4577	1.8554	0.4515	4.9049
1.2	1.9733	0.4245	5.5483	1.8778	0.4461	5.0248
1.4	1.9871	0.4216	5.6259	1.8978	0.4414	5.1318

TABLE 6

Characteristics of coupled line on PTFE cloth versus frequency with b = 7.00 mm, h_1 = 0.5 mm, h_2 = 3.0 mm, w = 0.5 mm, s = 1.5 mm, and θ = 0°.

Freq.	β^e	λ_g^e	ε_{eff}^e	β^o	λ_g^o	ε_{eff}^o
5.00	0.1490	0.7024	2.0265	0.1445	0.7245	1.9052
10.0	0.2994	0.6995	2.0438	0.2894	0.7238	1.9089
15.0	0.4515	0.6957	2.0657	0.4348	0.7226	1.9152
20.0	0.6052	0.6921	2.0876	0.5809	0.7210	1.9236
25.0	0.7600	0.6888	2.1073	0.7281	0.7191	1.9337
30.0	0.9158	0.6861	2.1244	0.8763	0.7169	1.9453
35.0	1.0722	0.6837	2.1394	1.0257	0.7146	1.9580
40.0	1.2291	0.6815	2.1527	1.1763	0.7122	1.9716

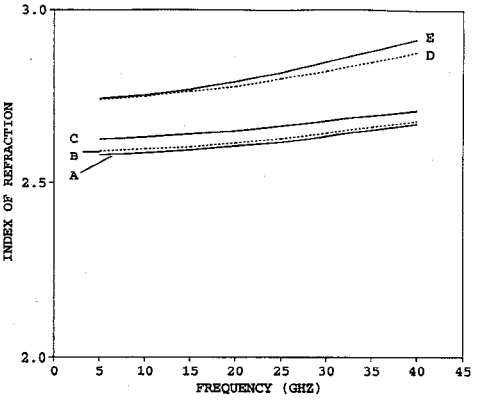

Fig. 5. Effective index of refraction versus frequency of grounded slotline with b = 1.0 mm, h_1 = 0.1 mm, h_2 = 0.4 mm, and w_1 =0.1 mm

(A) $\varepsilon_{xx} = \varepsilon_{yy} = \varepsilon_{zz}$ = 9.2 and $\mu_{xx} = \mu_{yy} = \mu_{zz}$ = 1.0.

(B) ε_{xx} = 9.2, $\varepsilon_{yy} = \varepsilon_{zz}$ = 10.1, and $\mu_{xx} = \mu_{yy} = \mu_{zz}$ = 1.0.

(C) ε_{xx} = 9.2, ε_{yy} = 13.6, ε_{zz} = 10.1, and $\mu_{xx} = \mu_{yy} = \mu_{zz}$ = 1.0.

(D) ε_{xx} = 9.2, ε_{yy} = 10.1, ε_{zz} = 11.6, μ_{xx} = 1.0, and $\mu_{yy} = \mu_{zz}$ = 1.2.

(E) ε_{xx} = 9.2, ε_{yy} = 10.1, ε_{zz} = 11.6, μ_{xx} =1.0, μ_{yy} = 1.2, and μ_{zz} = 1.97.